# First Introduction of an Azulenyl Group into the Bismuth and Antimony Center. Synthesis and Structure of Azulenylbismuthanes and Their Difluorides

A. F. M. Mustafizur Rahman, Toshihiro Murafuji,* Kei Kurotobi, and Yoshikazu Sugihara*

*Department of Chemistry, Faculty of Science, Yamaguchi University, Yamaguchi 753-8512, Japan*

Nagao Azuma

*Department of Chemistry, Faculty of Science, Ehime University, Matsuyama 790-8577, Japan*

*Received April 12, 2004*

A nonalternant organyl ligand derived from azulene, a 1,3-dichloro-2-azulenyl group, is introduced for the first time into the bismuth and antimony center. Conversion of the azulenylbismuthanes into the pentacoordinated difluorides by xenon difluoride promotes the $\pi$-polarization of the azulene nucleus, which is detected as a color change in solution as well as changes in the chemical shifts of the $^{13}C$ NMR spectra. A similar tendency is observed in the antimony congeners. The X-ray crystallographic study of (1,3-dichloro-2-azulenyl)-diphenylbismuth difluoride (**20b**) reveals that intermolecular $\pi-\pi$ stacking takes place between the azulenyl groups through the interaction of the five-membered ring with the seven-membered ring. This may reflect the more polarized azulenyl group of the difluorides, which strengthens the stacking interaction.



## Introduction

Construction of organometallics based on nonalternant conjugation has been receiving increasing interest.[1] Formation of a $\sigma$- or $\pi$-type coordinate bond between a metal center and nonalternant ligands is considered to endow molecules with a significant change of the properties that are markedly different from those given by the coordination of alternant ligands since the resonance stabilization of nonalternant conjugation is smaller than that of alternant conjugation.[2] Thus, we have revealed a unique structure of boron complex **1** comprised of nonalternant 8-methylamino-3-phenyl-1-azaazulene, in which the nonalternant conjugation in the 1-azaazulene skeleton is destroyed through the intramolecular boron−nitrogen coordinate bond.[1d]

Azulene, a nonalternant hydrocarbon and isomer of alternant naphthalene, is physicochemically characterized by high electron affinity, low ionization potential, and low aromatic resonance energy, together with the dipole moment vector whose negative end is toward its five-membered ring (Scheme 1). Despite such uniqueness of the electronic structure, the organometallic species bearing an azulenyl group as a ligand of the metal center have been very limited. In particular, there are few examples of the $\sigma$-type species,[3] although azulenes are known to coordinate with transition metal centers to form a $\pi$-complex.[1a,b,4] The reason is attributed to the lack of suitable methods for preparing $\sigma$-anions such as azulenyllithium or azulenyl-Grignard

**Chart 1**

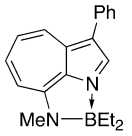


**1**

**Scheme 1**

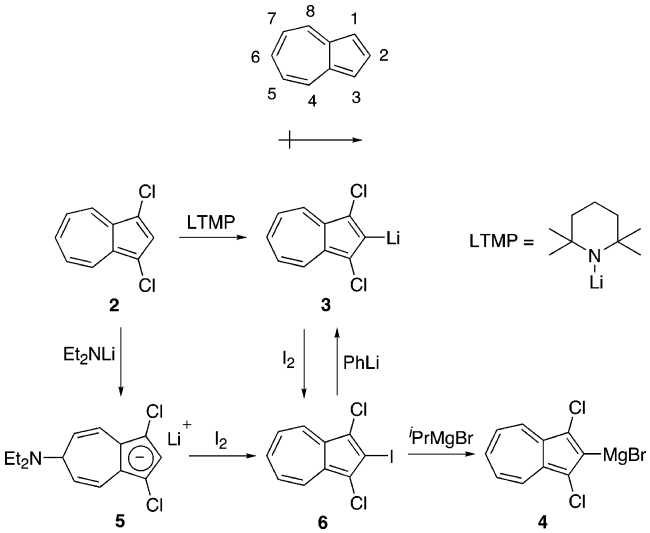


(1) (a) Matsubara, K.; Ryu, K.; Maki, T.; Iura, T.; Nagashima, H. *Organometallics* **2002**, *21*, 3023. (b) Arce, A. J.; De Sanctis, Y.; Galarza, E.; Garland, M. T.; Gobetto, R.; Machado, R.; Manzur, J.; Russo, A.; Spodine, E.; Stchedroff, M. J. *Organometallics* **2001**, *20*, 359. (c) Nitta, M.; Mitsumoto, Y.; Yamamoto, H. *J. Chem. Soc., Perkin Trans. 1* **2001**, 1901. (d) Sugihara, Y.; Murafuji, T.; Abe, N.; Takeda, M.; Kakehi, A. *New J. Chem.* **1998**, 1031.

(2) (a) Dewer, M. J. S.; De Llano, C. *J. Am. Chem. Soc.* **1969**, *91*, 789. (b) Sugihara, Y.; Hashimoto, R.; Fujita, H.; Abe, N.; Yamamoto, H.; Sugimura, T.; Murata, I. *J. Chem. Soc., Perkin Trans. 1* **1995**, 2813.

10.1021/om040053f CCC: $27.50 
Publication on Web 11/23/2004

**Scheme 2**

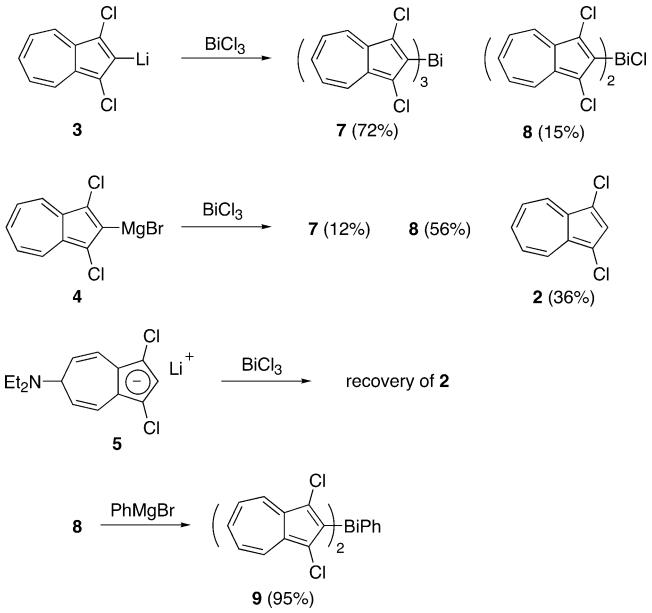


**Scheme 3**

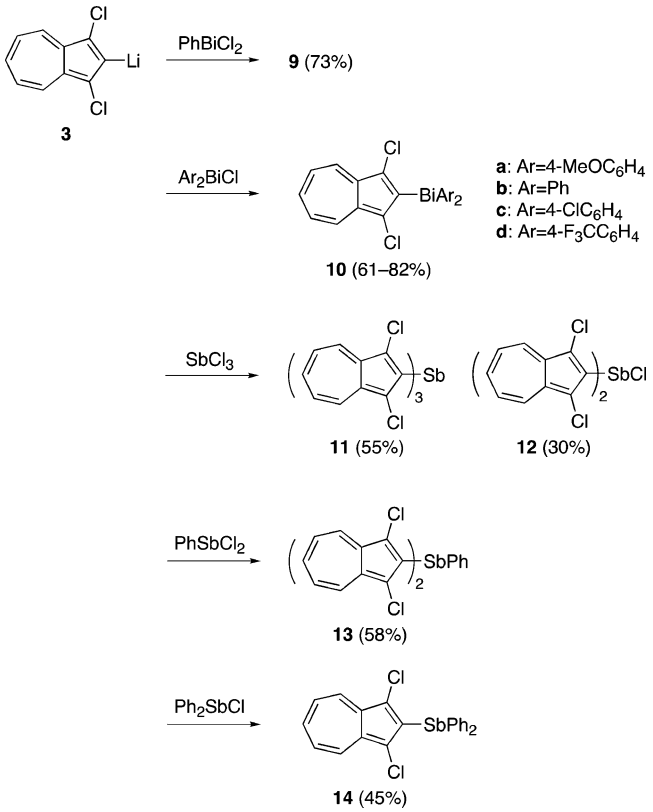


reagents, the generation of which has so far not been achieved. Very recently, we were successful for the first time in generating $\sigma$-anions **3** and **4**, starting from 1,3-dichloroazulene **2** (Scheme 1).[5] Herein, we report the first introduction of an azulenyl group into the bismuth center, that is, the synthesis and structural characterization of azulenylbismuthanes **7**−**10** and their difluorides **18**−**20**, together with their antimony congeners.

## Results and Discussion

**Synthesis of Azulenylbismuthanes and their Homologues of Antimony.** To know the difference in reactivity among anionic species **3**−**5**, we initially tried the reaction of the respective anions (ca. 3 equiv) with bismuth(III) chloride (1 equiv). When azulenyllithium **3** was allowed to react with bismuth(III) chloride, bismuthane **7** preferentially formed together with minor chlorobismuthane **8** in 72 and 15% yields [based on bismuth(III) chloride], respectively (Scheme 2). In contrast, the distribution of **7** and **8** was reversed when azulenyl-Grignard **4** was used. Thus, **8** formed as a main product (56%) along with **7** (12%), and in addition, **2** was obtained in 36% yield (based on **6**), reflecting the lowered nucleophilicity of **4**. An attempted reaction of $\pi$-anion **5** resulted in the complete recovery of **2**. The diethylamino group of **5** seems to coordinate with Lewis acidic bismuth(III) chloride to promote the elimination of this group from the azulene nucleus since the $\pi$-anion reacts with iodine to produce **6** in moderate yield. These results clarify the efficiency of **3** for the bismuth−carbon bond formation. Despite the reactive bismuth−chlorine bond, **8** is resistant to aqueous workup, although chlorobismuthanes are usually sensitive toward hydrolysis at the bismuth atom. The structure of **8** was confirmed by the reaction with phenylmagnesium bromide giving **9**.

Dichloro- and chlorobismuthanes underwent substitution smoothly with **3** to afford the corresponding mixed bismuthanes **9** and **10**, respectively (Scheme 3). Next, azulenyllithium **3** was applied to the reaction with an electrophile of the group 15 homologue. When antimony(III) chloride was allowed to react with **3**, unlike the case of bismuth(III) chloride, the ratio of chlorostibine **12** relative to **11** considerably increased, reflecting the difference of the Lewis acidity between the bismuth and antimony atoms. Similar reaction with dichloro- and chlorostibines[6] afforded the corresponding stibines **13** and **14**.

**Halogenation.** Triarylbismuthanes undergo preferential halogenation at the bismuth atom with sulfuryl chloride or xenon difluoride to give triarylbismuth dihalides in high yields. Unlike the aryl groups of benzenoid hydrocarbon, the azulenyl groups of **7** are considered to be reactive toward halogenation since the azulene nucleus undergoes electrophilic substitution at the five-membered ring (1- and 3-positions) and suffers from nucleophilic addition at the seven-membered ring (4-, 6-, and 8-positions) owing to the $\pi$-polarization. A preliminary reaction of **2** with sulfuryl chloride (1 equiv) in THF at 0 °C immediately produced brown, intractable substances and a small amount of **2** remained (confirmed by TLC), suggesting destruction of the conjugation in the azulene nucleus by sequential chlorination. When **7** was allowed to react with sulfuryl chloride under the same conditions, however, no such tendency

(3) (a) Kurotobi, K.; Tabata, H.; Miyauchi, M.; Murafuji, T.; Sugihara, Y. *Synthesis* **2002**, 1013. (b) Kurotobi, K.; Miyauchi, M.; Takakura, K.; Murafuji, T.; Sugihara, Y. *Eur. J. Org. Chem.* **2003**, 3663. (c) Ito, S.; Okujima, T.; Morita, N. *J. Chem. Soc., Perkin Trans. 1* **2002**, 1896.

(4) Edelmann, F.; Behrens, U. *Chem. Ber.* **1978**, *111*, 3001.

(5) Kurotobi, K.; Tabata, H.; Miyauchi, M.; Mustafizur Rahman, A. F. M.; Migita, K.; Murafuji, T.; Sugihara, Y.; Shimoyama, H.; Fujimori, K. *Synthesis* **2003**, 30.

(6) Nunn, M.; Sowerby, D. B.; Wesolek, D. M. *J. Organomet. Chem.* **1983**, *251*, C45.

**Scheme 4**

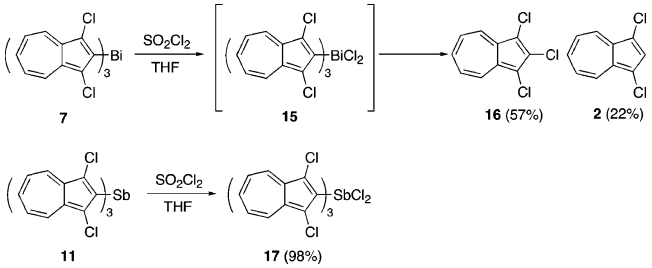


**Scheme 5**

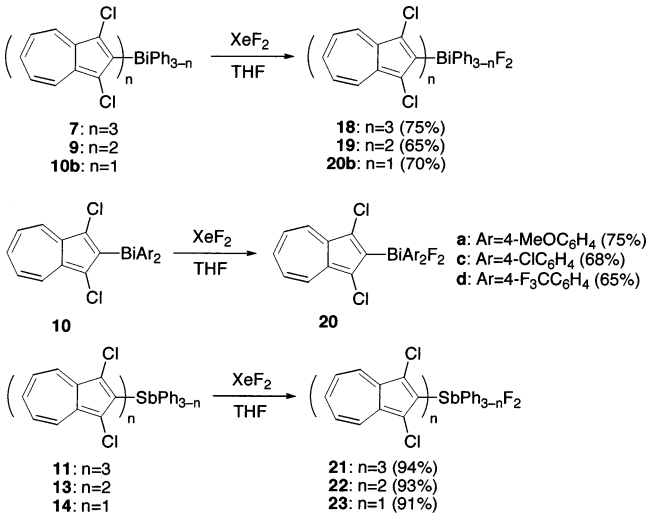


was observed. Thus, the reaction proceeded quickly (within 5 min), and a greenish product considered to be **15** was confirmed by TLC together with 1,2,3-trichloroazulene **16** and **2** (Scheme 4). Isolation of the product failed owing to decomposition in solution. Eventually, most of the azulenyl groups were recovered in the form of **16** and **2** (57 and 22% yields, respectively). In contrast, when **11** was chlorinated similarly, the color of the solution immediately changed from greenish blue to deep green, giving dichloride **17** quantitatively. These results show that the chlorination of the lone pair on the bismuth and antimony atoms precedes that of the azulene nucleus. Furthermore, dichloride **15** is thermally less stable and easily suffers from decomposition through the fission of the bismuth−carbon bonds. It is known that the geometry of triarylbismuth difluorides is much more stabilized than that of triarylbismuth dichlorides due to the apicophilicity of the more electronegative fluorine atoms in the apical positions of the trigonal bipyramidal structure. On adding xenon difluoride to a solution of **7** in THF, a color change similar to that observed in the chlorination of **11** took place and green solids of difluoride **18** gradually separated out (Scheme 5). Compound **18** is thermally stable in both solid and solution. The $^{19}$F NMR spectrum of **18** showed that the signal due to the fluorine atoms appears at $\delta_F$ −88.30 in DMSO-$d_6$, which caused confusion when compared with the value of triphenylbismuth difluoride ($\delta_F$ −153.28) in the same solvent. To know the reason for such a marked difference, bismuthanes **9** and **10** were similarly fluorinated and **19** and **20** were characterized by their $^{19}$F NMR spectra. Comparison of **19** with **20b** revealed that the fluorine signals showed an upfield shift with a decrease in the number of the azulenyl groups (−117.95 and −139.85 ppm in **19** and **20b**, respectively), while those of **20** were little affected by the *p*-substituents. Such behavior of **18** may be ascribed to the anisotropic effect of the chlorine atoms. Comparison of **18** with **7** by UV/vis spectroscopy in chloroform revealed that the absorbance ($\epsilon$) of the longest wavelength absorption band ($\lambda_{max}$ = ca. 640 nm) due to the charge transfer absorption of the azulene nucleus is larger in **18** (1540) than in **7** (1210). This tendency was commonly observed through the comparison of the difluorides with the parent bismuthanes and, furthermore, through the comparison of **11** with **17**. The $\epsilon$ value of **8** was approximately comparable to that of **9** (890 and 830, respectively). This indicates that the polarization of the azulene nucleus is enhanced in the higher oxidation state of the metal center.[7] To know the influence of the metal center on the polarization, antimony congeners **21**−**23** were synthesized and their $\epsilon$ values were compared with those of **18**, **19**, and **20b**. The value of **21** (1500) is comparable to that of **18**, and this tendency is seen between **22** and **19** and between **23** and **20b**. The values of stibines **11**−**14** are close to those of the bismuth congeners. These findings suggest that the electronic effect of the antimony center is quite similar to that of the bismuth center.

**$^{13}$C NMR Study.** Table 1 shows the chemical shifts ($\delta_C$) of ring carbons of azulenylbismuthanes **7**−**10** and their difluorides together with those of **2**. An outstanding spectroscopic feature is in the chemical shifts of the azulene nucleus. The C1 signals of **10** exhibited downfield shift with increasing electron-withdrawing ability of the *p*-substituents, suggesting the inductive effect by the aryl groups. The signals due to the seven-membered ring carbons of the bismuthanes showed chemical shifts almost identical to those of **2**. In contrast, the azulene ring carbons of **20** were little affected by the *p*-substituents but were governed by the effect of introduction of the fluorine atoms. Thus, the signals due to the C1 and C2 atoms appeared more upfield, while those due to the seven-membered ring carbons were observed more downfield, relative to the parent **10**. Interestingly, the tendency of the downfield shift was marked in the C4 and C6 atoms rather than in the C5 atoms. These findings clarify the change in the conjugation of the azulene nucleus accompanied by the change in the geometry of the bismuth atom. Namely, the $\pi$-polarization of the azulene nucleus is pronounced in **20** compared to the parent **10**. This is in good accord with the finding deduced from the UV/vis studies of these compounds. The upfield shifts of the C1′ and C2′ atoms and the downfield shift of the C3′ and C4′ atoms in **20** show the $\pi$-polarization in the benzene rings.[8] Table 2 shows the chemical shifts ($\delta_C$) of ring carbons of azulenylstibines. A similar tendency was observed in the antimony congeners. Except for the ipso carbons, the chemical shifts of the antimony derivatives are quite similar to those of the bismuth congeners.

(7) The coordination number−photophysical property relationships for the tri(9-anthryl)derivatives of boron, silicon, phosphorus, and bismuth, see: (a) Yamaguchi, S.; Akiyama, S.; Tamao, K. *J. Am. Chem. Soc.* **2000**, *122*, 6335. (b) Yamaguchi, S.; Akiyama, S.; Tamao, K. *J. Am. Chem. Soc.* **2001**, *123*, 11372. (c) Yamaguchi, S.; Akiyama, S.; Tamao, K. *J. Am. Chem. Soc.* **2000**, *122*, 6793. (d) Yamaguchi, S.; Akiyama, S.; Tamao, K. *J. Organomet. Chem.* **2002**, *646*, 277. (e) Yamaguchi, S.; Shirasaka, T.; Tamao, K. *Organometallics* **2002**, *21*, 2555.

**Table 1. $^{13}$C NMR Spectral Data of Azulenylbismuthanes and Difluorides in DMSO-$d_6$**

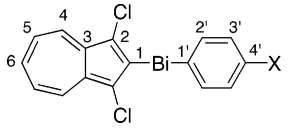


| | C1 | C2 | C3 | C4 | C5 | C6 | C1′ | C2′ | C3′ | C4′ |
|---|---|---|---|---|---|---|---|---|---|---|
| **2** | 132.56 | 113.16 | 132.56 | 135.73 | 124.69 | 141.73 | | | | |
| **7** | *a* | 122.88 | 133.00 | 134.62 | 124.51 | 141.23 | | | | |
| **8** | *a* | 121.50 | 133.68 | 133.87 | 124.04 | 140.30 | | | | |
| **9** | 165.10 | 122.42 | 133.23 | 134.21 | 124.38 | 140.89 | 156.58 | 139.80 | 130.23 | 127.94 |
| **10a**[b] | 164.08 | 122.64 | 133.33 | 134.01 | 124.27 | 140.76 | 147.12 | 139.73 | 116.29 | 159.07 |
| **10b** | 165.40 | 122.64 | 133.39 | 134.13 | 124.29 | 140.81 | 157.45 | 138.39 | 130.36 | 127.68 |
| **10c** | 167.22 | 122.44 | 133.49 | 134.25 | 124.27 | 140.98 | 157.11 | 140.35 | 130.30 | 132.84 |
| **10d**[c] | 168.81 | 122.40 | 133.60 | 134.40 | 124.50 | 141.09 | 165.20 | 139.24 | 126.50 | 128.23 |
| **19**[d] | *a* | 116.50 | 132.40 | 139.01 | 126.67 | 144.97 | *a* | 135.26 | 132.20 | 132.98 |
| **20a**[b,d] | 158.57 | 116.35 | 132.30 | 138.49 | 126.41 | 144.47 | 144.08 | 135.25 | 117.21 | 162.27 |
| **20b**[d] | 159.22 | 116.42 | 132.39 | 138.60 | 126.54 | 144.57 | 154.59 | 133.93 | 132.01 | 132.50 |
| **20c**[d] | 158.88 | 116.56 | 132.37 | 138.57 | 126.48 | 144.61 | 154.62 | 135.35 | 131.53 | 137.32 |
| **20d**[c,d] | 159.80 | 116.84 | 132.48 | 138.45 | 126.43 | 144.55 | 162.80 | 134.47 | 128.25 | 131.98 |

[a] Not observed. [b] The chemical shift of the methyl carbon: $\delta$ 54.98 (**10a**) and 55.97 (**20a**). [c] $J_{CF}$ = around 3.7(q), 32(q), and 273(q) for C3′, C4′, and $CF_3$, respectively. The chemical shift of the $CF_3$ carbon: $\delta$ 124.72 (**10d**) and 123.81 (**20d**). [d] The $^2J_{CF}$ and $^3J_{CF}$ couplings of the fluorine atoms attached to the bismuth atom were not detected in the azulenyl and phenyl ring carbons.

**Table 2. $^{13}$C NMR Spectral Data of Azulenylstibines and Difluorides in DMSO-$d_6$**

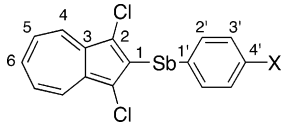


| | C1 | C2 | C3 | C4 | C5 | C6 | C1′ | C2′ | C3′ | C4′ |
|---|---|---|---|---|---|---|---|---|---|---|
| **11** | 140.18 | 121.48 | 132.46 | 135.20 | 124.88 | 142.16 | | | | |
| **13** | 141.88 | 120.94 | 132.62 | 134.91 | 124.81 | 142.78 | 134.30 | 137.46 | 128.78 | 129.26 |
| **14** | 141.95 | 121.25 | 132.84 | 135.02 | 124.82 | 143.64 | 136.49 | 136.39 | 128.95 | 128.89 |
| **21**[a] | 137.19 | 117.42 | 132.65 | 138.80 | 126.29 | 145.02 | | | | |
| **23**[b] | 139.43 | 116.22 | 132.45 | 138.26 | 126.16 | 144.48 | 133.10 | 135.25 | 130.25 | 133.03 |

[a] The $^2J_{CF}$ and $^3J_{CF}$ couplings of the fluorine atoms attached to the antimony atom were not detected in the azulenyl and phenyl ring carbons. [b] $^2J_{CF}$ = 13.9(t) for the C1′ and $^3J_{CF}$ = 4.6(t) for the C2′.

**X-ray Structure Analysis of Bismuthane 7 and Difluoride 20b.** To know how the azulenyl group attached to the bismuth(III) and -(V) centers behaves in solid, X-ray structure analysis was carried out for **7** and **20b** (Tables 3 and 4 and Figures 1−3). The bismuth center of **7** has a pyramidal configuration (Figure 1) and is surrounded by the six chlorine atoms with distances of 3.493(6)−4.033(5) Å, which are all within the sum of the van der Waals radii (4.04 Å). The partially larger bond angles around the bismuth center are due to the steric bulkiness of the azulenyl groups. The enhanced stability of chlorobismuthane **8** may be mainly attributed to the intramolecular interaction and kinetic stabilization by these chlorine atoms. The bismuth center of **20b** possesses a trigonal bipyramidal geometry with the fluorine atoms and the carbon atoms of the azulenyl and phenyl groups in the apical and equatorial positions, respectively (Figure 2). An outstanding structural feature is seen in the crystal structure of **20b**. An intermolecular $\pi-\pi$ stacking is observed between the azulenyl groups[9] through the interaction of the five-membered ring with the seven-membered ring, with the shortest interatomic distance of 3.54(2) Å between the C4 and C9 atoms (Figure 3). While the azulenyl group is approximately coplanar with the equatorial plane [C2−C1−Bi−C17 = 166(1)°], the two phenyl groups lie perpendicular to this plane as if they surround the azulenyl groups of the neighboring molecules. This

**Table 3. Selected Bond Lengths (Å) and Angles (deg) for 7 and 20b**

| **7** | | **20b** | |
|---|---|---|---|
| Bi−C(1) | 2.23(2) | Bi−C(1) | 2.15(2) |
| Bi−C(11) | 2.27(2) | Bi−C(11) | 2.19(2) |
| Bi−C(21) | 2.26(2) | Bi−C(17) | 2.19(2) |
| | | Bi−F(1) | 2.27(1) |
| | | Bi−F(2) | 2.189(9) |
| C(1)−C(2) | 1.38(2) | C(1)−C(2) | 1.40(2) |
| C(2)−C(3) | 1.41(3) | C(2)−C(3) | 1.40(2) |
| C(3)−C(4) | 1.41(3) | C(3)−C(4) | 1.42(2) |
| C(3)−C(9) | 1.50(3) | C(3)−C(9) | 1.47(2) |
| C(4)−C(5) | 1.39(3) | C(4)−C(5) | 1.31(2) |
| C(5)−C(6) | 1.33(3) | C(5)−C(6) | 1.32(3) |
| C(6)−C(7) | 1.33(3) | C(6)−C(7) | 1.44(3) |
| C(7)−C(8) | 1.38(3) | C(7)−C(8) | 1.41(2) |
| C(8)−C(9) | 1.39(3) | C(8)−C(9) | 1.36(2) |
| C(9)−C(10) | 1.38(3) | C(9)−C(10) | 1.39(2) |
| C(1)−C(10) | 1.42(2) | C(1)−C(10) | 1.37(2) |
| C(1)−Bi−C(11) | 92.6(6) | C(1)−Bi−C(11) | 115.5(6) |
| C(1)−Bi−C(21) | 99.2(7) | C(1)−Bi−C(17) | 117.4(6) |
| C(11)−Bi−C(21) | 100.6(6) | C(11)−Bi−C(17) | 127.1(6) |
| | | F(1)−Bi−F(2) | 178.5(4) |

(8) $\pi$-Polarization is observed in diaryltrifluorosilicates. Thus, the ipso carbons attached to the pentacoordinate silicon appear more downfield compared to those of the parent tetracoordinate silanes. This is attributed to the $\pi$-inductive effect induced by the electronic fields of the charged substituents. The upfield shift of the ipso carbons in the pentacoordinate antimony and bismuth halides may be ascribed to this $\pi$-inductive effect. For the $\pi$-polarization of the silicates, see: Tamao, K.; Hayashi, T.; Ito, Y. *Organometallics* **1992**, *11*, 182.

(9) Sterically protected phosphaethenes bearing an azulenyl group at the ethene carbon, see: Yasunami, M.; Ueno, T.; Yoshifuji, M.; Okamoto, A.; Hirotsu, K. *Chem. Lett.* **1992**, 1971.

**Table 4. Crystallographic Parameters for 7 and 20b**

| | **7**·THF | **20b** |
|---|---|---|
| empirical formula | $C_{34}H_{23}BiCl_6O$ | $C_{22}H_{15}BiCl_2F_2$ |
| fw | 869.25 | 597.24 |
| color, habit | green, prismatic | green, prismatic |
| cryst dimens (mm) | 0.33 × 0.28 × 0.18 | 0.25 × 0.13 × 0.13 |
| cryst syst | monoclinic | monoclinic |
| $a$ (Å) | 12.063(6) | 8.030(6) |
| $b$ (Å) | 21.085(7) | 16.78(1) |
| $c$ (Å) | 12.721(7) | 15.44(2) |
| $\beta$ (deg) | 92.81(4) | 97.2(1) |
| $V$ (Å$^3$) | 3231(2) | 2064(3) |
| space group | $P2_1/n$ (#14) | $P2_1/c$ (#14) |
| $Z$ | 4 | 4 |
| $D_{calc}$ (g cm$^{-3}$) | 1.786 | 1.922 |
| $F_{000}$ | 1680.00 | 1128.00 |
| $\mu$(Mo K$\alpha$) (cm$^{-1}$) | 59.69 | 88.06 |
| $2\theta_{max}$ (deg) | 55.0 | 55.4 |
| scan rate (deg min$^{-1}$) | 32.0 | 8.0 |
| scan width (deg) | 1.47 + 0.30 tan $\theta$ | 1.52 + 0.30 tan $\theta$ |
| no. of rflns measd total; unique | 7991; 7428 | 5263; 4749 |
| no. of observns | 5078 ($I > 0.00\sigma(I)$) | 2953 ($I > 0.00\sigma(I)$) |
| no. of variables | 369 | 244 |
| residuals: $R$;[a] $R_w$[b] | 0.141; 0.191 | 0.096; 0.117 |
| goodness of fit indicator | 1.01 | 1.18 |
| max. shift/error in final cycle | 0.001 | 0.000 |
| max. and min. peaks in final diff map (e$^-$/Å$^3$) | 4.01; −3.85 | 2.11; −2.19 |

[a] $R = \sum(F_o^2 - F_c^2)/\sum F_o^2$. [b] $R_w = [\sum w(F_o^2 - F_c^2)^2/\sum w(F_o^2)^2]^{1/2}$; $w = 1/\sigma^2(F_o^2)$.

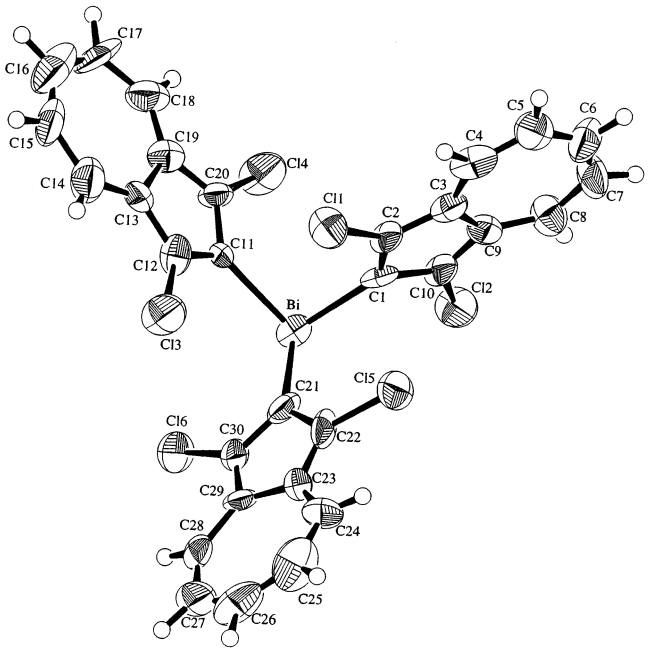


**Figure 1.** ORTEP drawing of **7** showing the atomic numbering scheme. The thermal ellipsoids are drawn at the 50% probability level. A THF molecule is omitted for clarity.

stacking interaction was not observed in **7**, although the bismuth center possesses three azulenyl groups. The difference in the crystal structures of **7** and **20b** may reflect the enhanced polarization in the azulene nucleus of the latter, which strengthens the stacking interaction.

In conclusion, this work shows a potential utility of nonalternant azulenes not only as $\sigma$-ligands of the metal center but also as key building blocks for the construction of supramolecular systems composed of organometallics based on the $\pi-\pi$ interaction.

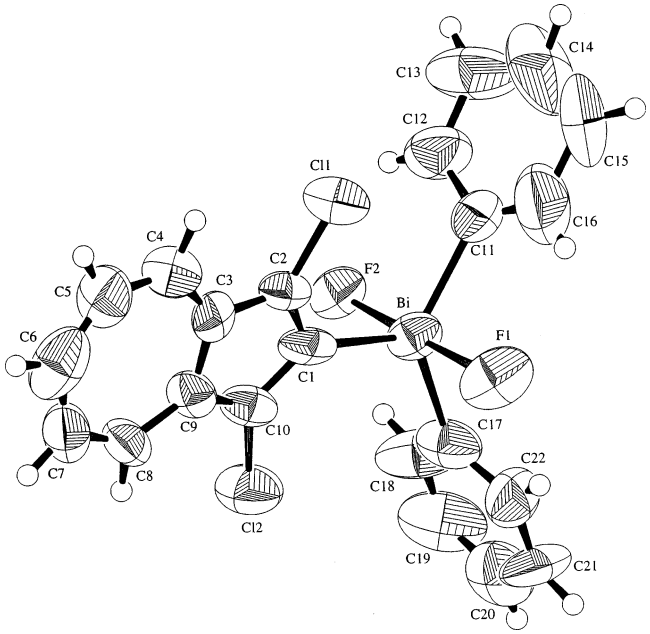


**Figure 2.** ORTEP drawing of **20b** showing the atomic numbering scheme. The thermal ellipsoids are drawn at the 50% probability level.

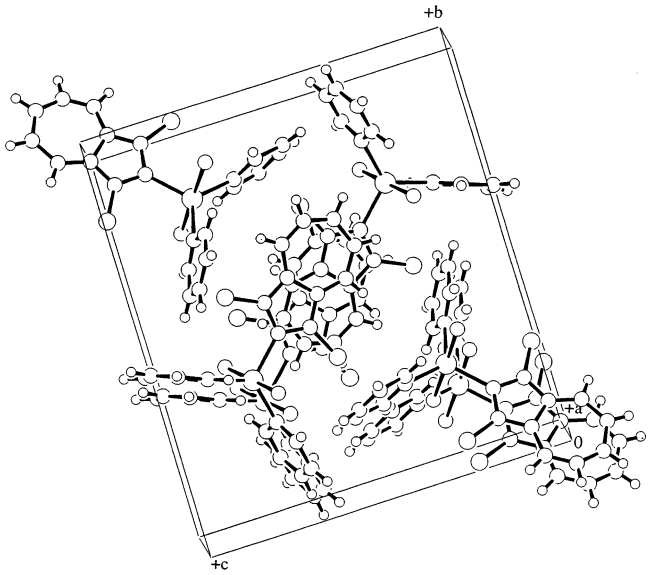


**Figure 3.** Crystal structure of **20b**.

## Experimental Section

**General Comments.** All reactions were carried out under argon unless otherwise noted. THF and diethyl ether were distilled from calcium hydride under nitrogen before use. Bismuth(III) chloride and antimony(III) chloride were purified by refluxing with thionyl chloride. $^1$H and $^{13}$C NMR spectra were recorded in $CDCl_3$ or DMSO-$d_6$ on a Bruker AVANCE 400S spectrometer with TMS as an internal standard. $^{19}$F NMR spectra were measured in DMSO-$d_6$ on a Bruker AVANCE 400S spectrometer with benzotrifluoride ($\delta_F$ −64.0) as an internal standard. UV/vis spectra were measured in $CHCl_3$ by means of a Shimadzu UV-1600PC spectrophotometer. 1,3-Dichloroazulene **2** was synthesized by the chlorination of azulene with NCS.

**1,3-Dichloroazulene (2):** blue solids; yield 85%; mp 85−87 °C (lit.[10] 85−87 °C); $^1$H NMR ($CDCl_3$) $\delta$ 7.18 (2H, t, $J$ 10.0),

(10) Anderson, A. G., Jr.; Nelson, J. A.; Tazuma, J. J. *J. Am. Chem. Soc.* **1953**, *75*, 4980.

7.64 (1H, t, *J* 9.9), 7.65 (1H, s), 8.32 (2H, d, *J* 9.3); UV/vis ($CHCl_3$) $\lambda_{max}$/nm ($\epsilon$) 241 (20420), 288 (34140), 294 (29410), 344 (3360), 352 (4520), 361 (3000), 369 (5030), 642 (380).

**Generation of Azulenyllithium 3 and the Reaction with Electrophiles. General Procedure.** A typical example is exemplified by the reaction with bismuth(III) chloride. To a solution of lithium 2,2,6,6-tetramethylpiperidide (ca. 4.5 mmol) prepared from 2,2,6,6-tetramethylpiperidine (4.5 mmol) and BuLi (4.5 mmol) in THF (5 mL) at −70 °C was added a solution of **2** (3.0 mmol) in THF (3 mL) at the same temperature. The color of the solution immediately turned from blue to dark green, showing the generation of **3**. To this solution thus obtained was added a solution of bismuth(III) chloride (1.0 mmol) in THF (5 mL), and the resulting solution was stirred for 5 min. The reaction was quenched at −70 °C with brine (10 mL), and the green precipitate was separated by filtration. The filtrate was extracted with ethyl acetate (7 mL × 3), and the combined extracts were dried over anhydrous sodium sulfate and evaporated to leave a residue, which was recrystallized from THF−MeOH (5:1) to give pure **7**. The precipitate was recrystallized from THF−MeOH (5:1) to give **8**. Yields are based on bismuth(III) chloride.

**1,3-Dichloro-2-iodoazulene (6):**[5] blue solids; yield 95%; mp 102−103 °C; $^1$H NMR ($CDCl_3$) $\delta$ 7.22 (2H, t, *J* 10.0), 7.69 (1H, t, *J* 9.9), 8.35 (2H, d, *J* 10.2); $^{13}$C NMR ($CDCl_3$) $\delta$ 103.78, 119.58, 124.60, 132.44, 134.66, 140.09. Anal. Calcd for $C_{10}H_5Cl_2I$: C, 37.19; H, 1.56. Found: C, 37.41; H, 1.50.

**Tris(1,3-dichloro-2-azulenyl)bismuthane (7):** green solids; yield 72%; mp 258−259 °C; $^1$H NMR (DMSO-$d_6$) $\delta$ 7.30 (6H, t, *J* 9.9), 7.77 (3H, t, *J* 9.9), 8.22 (6H, d, *J* 9.3); UV/vis ($CHCl_3$) $\lambda_{max}$/nm ($\epsilon$) 242 (50 870), 313 (147 290), 348 (26 660), 365 (31 320), 645 (1210). Anal. Calcd for $C_{30}H_{15}BiCl_6$: C, 45.20; H, 1.90. Found: C, 45.44; H, 2.02.

**Chlorobis(1,3-dichloro-2-azulenyl)bismuthane (8):** green solids; yield 15%; mp 251−252 °C; $^1$H NMR (DMSO-$d_6$) $\delta$ 7.17 (4H, t, *J* 9.8), 7.66 (2H, t, *J* 9.8), 7.96 (4H, d, *J* 9.8); UV/vis ($CHCl_3$) $\lambda_{max}$/nm ($\epsilon$) 242 (38 070), 295 (70 100), 300 (69 690), 315 (77 320), 345 (13 810), 352 (sh, 14 160), 361 (16 880), 645 (890). Elemental analysis of this compound failed due to its slow decomposition upon storage.

**Bis(1,3-dichloro-2-azulenyl)phenylbismuthane (9):** green solids; yield 73%; mp 206−207 °C; $^1$H NMR (DMSO-$d_6$) $\delta$ 7.27−7.32 (4H, m), 7.40 (2H, t, *J* 7.5, ArH), 7.77 (2H, t, *J* 9.8, AzH), 8.17 (2H, d, *J* 7.2, ArH), 8.20 (4H, d, *J* 9.8, AzH); UV/vis ($CHCl_3$) $\lambda_{max}$/nm ($\epsilon$) 241 (40 500), 309 (89 510), 349 (sh, 17 130), 365 (18 330), 642 (830). Anal. Calcd for $C_{26}H_{15}BiCl_4$: C, 46.05; H, 2.23. Found: C, 46.56; H, 1.94.

**1,3-Dichloro-2-azulenylbis(4-methoxyphenyl)bismuthane (10a):** green solids; yield 70%; mp 109−111 °C; $^1$H NMR (DMSO-$d_6$) $\delta$ 3.70 (6H, s), 6.95 (4H, d, *J* 8.4, ArH), 7.29 (2H, t, *J* 9.8, AzH), 7.76 (4H, d, *J* 8.4, ArH), 7.77 (1H, t, *J* 9.9, AzH), 8.21 (2H, d, *J* 9.7, AzH); UV/vis ($CHCl_3$) $\lambda_{max}$/nm ($\epsilon$) 243 (45 870), 300 (63 400), 307 (62 850), 349 (sh, 9420), 365 (8610), 642 (480). Anal. Calcd for $C_{24}H_{19}BiCl_2O_2$: C, 46.55; H, 3.09. Found: C, 47.08; H, 2.99.

**(1,3-Dichloro-2-azulenyl)diphenylbismuthane (10b):** green solids; yield 82%; mp 111−112 °C; $^1$H NMR (DMSO-$d_6$) $\delta$ 7.29 (2H, t, *J* 9.9, AzH), 7.29 (2H, t, *J* 7.3, ArH), 7.39 (4H, t, *J* 7.4, ArH), 7.78 (1H, t, *J* 9.9, AzH), 7.90 (4H, d, *J* 6.8, ArH), 8.21 (2H, d, *J* 9.5, AzH); UV/vis ($CHCl_3$) $\lambda_{max}$/nm ($\epsilon$) 240 (30 250), 299 (52 470), 307 (52 010), 364 (7620), 642 (400). Anal. Calcd for $C_{22}H_{15}BiCl_2$: C, 47.25; H, 2.70. Found: C, 47.15; H, 2.71.

**1,3-Dichloro-2-azulenylbis(4-chlorophenyl)bismuthane (10c):** green solids; yield 65%; mp 115−117 °C; $^1$H NMR (DMSO-$d_6$) $\delta$ 7.29 (2H, t, *J* 9.8, AzH), 7.42 (4H, d, *J* 8.3, ArH), 7.77 (1H, t, *J* 9.9, AzH), 7.89 (4H, d, *J* 8.3, ArH), 8.21 (2H, d, *J* 9.9, AzH); UV/vis ($CHCl_3$) $\lambda_{max}$/nm ($\epsilon$) 241 (38 110), 300 (sh, 52 060), 307 (52 860), 348 (sh, 7390), 363 (7930), 641 (420). Anal. Calcd for $C_{22}H_{13}BiCl_4$: C, 42.07; H, 2.09. Found: C, 42.36; H, 2.05.

**1,3-Dichloro-2-azulenylbis(4-trifluoromethylphenyl)bismuthane (10d):** green solids; yield 61%; mp 135−138 °C; $^1$H NMR (DMSO-$d_6$) $\delta$ 7.30 (2H, t, *J* 10.0, AzH), 7.71 (4H, d, *J* 7.9, ArH), 7.78 (1H, t, *J* 9.9, AzH), 8.15 (4H, d, *J* 7.9, ArH), 8.23 (2H, d, *J* 9.0, AzH); UV/vis ($CHCl_3$) $\lambda_{max}$/nm ($\epsilon$) 241 (25 820), 301 (43 360), 348 (5910), 362 (6710), 642 (380). Anal. Calcd for $C_{24}H_{13}BiCl_2F_6$: C, 41.46; H, 1.88. Found: C, 41.24; H, 1.97.

**Tris(1,3-dichloro-2-azulenyl)stibine (11):** green solids; yield 55%; mp 270−271 °C; $^1$H NMR (DMSO-$d_6$) $\delta$ 7.34 (6H, t, *J* 9.9), 7.82 (3H, t, *J* 9.9), 8.27 (6H, d, *J* 9.6); UV/vis ($CHCl_3$) $\lambda_{max}$/nm ($\epsilon$) 242 (48 130), 310 (158 500), 367 (25 880), 648 (1250). Anal. Calcd for $C_{30}H_{15}SbCl_6$: C, 50.76; H, 2.13. Found: C, 50.72; H, 2.15.

**Chlorobis(1,3-dichloro-2-azulenyl)stibine (12):** green solids; yield 30%; mp 264−265 °C; $^1$H NMR ($CDCl_3$) $\delta$ 7.17 (4H, t, *J* 9.0), 7.63 (2H, t, *J* 9.4), 8.28 (4H, d, *J* 9.6); due to low solubility, measurement of $^{13}$C NMR spectrum failed; UV/vis ($CHCl_3$) $\lambda_{max}$/nm ($\epsilon$) 242 (36 870), 308 (79 150), 364 (sh, 16 140), 648 (920). Anal. Calcd for $C_{20}H_{10}SbCl_5$: C, 43.73; H, 1.83. Found: C, 44.24; H, 1.85.

**Bis(1,3-dichloro-2-azulenyl)phenylstibine (13):** green solids; yield 58%; mp 195−198 °C; $^1$H NMR (DMSO-$d_6$) $\delta$ 7.31−7.36 (7H, m), 7.72 (2H, d, *J* 7.7, ArH), 7.81 (2H, t, *J* 9.8, AzH), 8.26 (4H, d, *J* 9.9, AzH); UV/vis ($CHCl_3$) $\lambda_{max}$/nm ($\epsilon$) 242 (32 320), 306 (68 090), 367 (sh, 14 900), 644 (820). Anal. Calcd for $C_{26}H_{15}SbCl_4$: C, 52.48; H, 2.56. Found: C, 52.84; H, 2.50.

**(1,3-Dichloro-2-azulenyl)diphenylstibine (14):** green solids; yield 45%; mp 133−135 °C; $^1$H NMR (DMSO-$d_6$) $\delta$ 7.32−7.37 (8H, m), 7.50−7.52 (4H, m), 7.83 (1H, t, *J* 9.9, AzH), 8.28 (2H, d, *J* 9.4, AzH); UV/vis ($CHCl_3$) $\lambda_{max}$/nm ($\epsilon$) 242 (27 360), 299 (46 720), 329 (14 690), 645 (430). Anal. Calcd for $C_{22}H_{15}SbCl_2$: C, 55.98; H, 3.20. Found: C, 56.31; H, 3.19.

**Generation of Azulenyl-Grignard 4 and the Reaction with Bismuth(III) Chloride.** To a solution of **6** (3.0 mmol) in THF (5 mL) was added at −30 °C a solution of *i*-PrMgBr (3.6 mmol) in THF (3 mL). The color of the solution turned from blue to bluish green, showing the generation of **4**. To this solution thus obtained was added a solution of bismuth(III) chloride (1.0 mmol) in THF (5 mL), and the resulting solution was stirred for 5 min. The reaction was quenched at −30 °C with brine (10 mL), and the green precipitate was separated by filtration. The precipitate was recrystallized from THF−MeOH (5:1) to give **8** in 56% yield. The filtrate was extracted with ethyl acetate (7 mL × 3), and the combined extracts were dried over anhydrous sodium sulfate and evaporated to leave a residue, which was recrystallized from THF−MeOH (5:1) to give pure **7** in 12% yield. Evaporation of the filtrate after filtration of **7** gave a residue, which was chromatographed (silica gel; hexane) to give **2** in 36% yield.

**Reaction of 8 with Phenylmagnesium Bromide.** To a solution of **8** (0.3 mmol) in THF (5 mL) was added at 0 °C a solution of phenylmagnesium bromide (ca. 0.6 mmol) in the same solvent (1 mL), and the reaction mixture was stirred for 3 h, during which time the temperature was raised to ambient. The reaction was quenched with brine (3 mL), and the resulting mixture was extracted with ethyl acetate (5 mL × 3). The combined extracts were dried over anhydrous sodium sulfate and evaporated to leave a residue, which was crystallized from MeOH to give **9** in 95% yield.

**Generation of Lithium 6-*N*,*N*-Diethylamino-6*H*-azulenate (5) and the Reaction with Bismuth(III) Chloride.** To a solution of lithium diethylamide (ca. 3.0 mmol), prepared from diethylamine (3.0 mmol) and BuLi (3.0 mmol) in ether (10 mL) at −20 °C, was added a solution of **2** (3.0 mmol) in ether (3 mL) at −70 °C. The color of the solution turned from blue to yellow, showing the generation of **5**. Then a solution of bismuth(III) chloride (1.0 mmol) in THF (5 mL) was added at this temperature. After 5 min the reaction was quenched at −70 °C with brine (10 mL) and the mixture was extracted

with ethyl acetate (7 mL × 3). The combined extracts were dried over anhydrous sodium sulfate and evaporated to leave a residue, from which **2** was recovered intact.

**Chlorination of 7 with Sulfuryl Chloride.** To a solution of **7** (1.0 mmol) in THF (10 mL) was added sulfuryl chloride (1.0 mmol) in dichloromethane (1.0 mL) at 0 °C, and the reaction mixture was stirred for 3 h, during which time the temperature was raised to ambient. The mixture was evaporated to leave an oily residue containing insoluble substances, which was extracted with hexane (7 mL × 3). The combined extracts were purified by silica gel column chromatography using hexane as eluent to give 1,3-dichloroazulene **2** (22%) and 1,2,3-trichloroazulene **16** (57%).

**1,2,3-Trichloroazulene (16):** blue solids; yield 57%; mp 136−137 °C (lit.[11] 137 °C); $^1$H NMR ($CDCl_3$) $\delta$ 7.28 (2H, t, $J$ 9.8), 7.66 (1H, t, $J$ 9.6), 8.30 (2H, d, $J$ 10.0); $^{13}$C NMR ($CDCl_3$) $\delta$ 112.38, 124.81, 131.86, 134.44 (× 2), 139.58. Anal. Calcd for $C_{10}H_5Cl_3$: C, 51.88; H, 2.18. Found: C, 51.84; H, 2.25.

**Chlorination of 11 with Sulfuryl Chloride.** To a solution of **11** (1.0 mmol) in THF (10 mL) was added sulfuryl chloride (1.0 mmol) in dichloromethane (1.0 mL) at 0 °C, and the reaction mixture was stirred for 3 h, during which time the temperature was raised to ambient. The mixture was evaporated to leave solids, which were crystallized from hexane−AcOEt (5:1) to give pure **17**.

**Tris(1,3-dichloro-2-azulenyl)antimony dichloride (17):** green solids; yield 98%; mp 290−292 °C; $^1$H NMR (DMSO-$d_6$) $\delta$ 7.58 (6H, t, $J$ 9.9), 8.09 (3H, t, $J$ 10.3), 8.66 (6H, d, $J$ 9.6); due to low solubility, measurement of $^{13}$C NMR spectrum failed; UV/vis ($CHCl_3$) $\lambda_{max}$/nm ($\epsilon$) 241 (50 880), 313 (173 650), 355 (26 290), 371 (16 160), 648 (1610). Anal. Calcd for $C_{30}H_{15}SbCl_8$: C, 46.15; H, 1.94. Found: C, 46.16; H, 2.23.

**Fluorination of Azulenylbismuthanes with Xenon Difluoride. General Procedure.** A typical example is exemplified by the reaction of **7**. To a solution of **7** (1.0 mmol) in THF (15 mL) was added xenon difluoride (1.2 mmol) at 0 °C, and the mixture was stirred for 3 h. Evaporation of the resulting mixture gave a residue, which was crystallized from MeOH to give **18**.

**Tris(1,3-dichloro-2-azulenyl)bismuth difluoride (18):** green solids; yield 75%; mp 191−192 °C; $^1$H NMR (DMSO-$d_6$) $\delta$ 7.36 (6H, t, $J$ 9.9), 7.61 (3H, t, $J$ 9.9), 8.64 (6H, d, $J$ 9.3); $^{19}$F NMR (DMSO-$d_6$) $\delta$ −88.30 (s); due to low solubility, measurement of $^{13}$C NMR spectrum failed; UV/vis ($CHCl_3$) $\lambda_{max}$/nm ($\epsilon$) 241 (50 130), 311 (160 070), 346 (24 210), 351 (24 380), 368 (16 750), 645 (1540). Anal. Calcd for $C_{30}H_{15}BiCl_6F_2$: C, 43.15; H, 1.81. Found: C, 43.18; H, 1.76.

**Bis(1,3-dichloro-2-azulenyl)phenylbismuth difluoride (19):** green solids; yield 65%; mp 153−155 °C; $^1$H NMR (DMSO-$d_6$) $\delta$ 7.57 (4H, t, $J$ 10.0, AzH), 7.73 (1H, t, $J$ 7.4, ArH), 7.79 (2H, t, $J$ 9.6, AzH), 7.91 (2H, t, $J$ 7.7, ArH), 8.38 (2H, d, $J$ 7.5, ArH), 8.57 (4H, d, $J$ 9.5, AzH); $^{19}$F NMR (DMSO-$d_6$) $\delta$ −117.95 (s); UV/vis ($CHCl_3$) $\lambda_{max}$/nm ($\epsilon$) 241 (34 700), 309 (92 700), 345 (15 300), 351 (15 100), 642 (950). Anal. Calcd for $C_{26}H_{15}BiCl_4F_2$: C, 43.60; H, 2.11. Found: C, 43.23; H, 2.46.

**1,3-Dichloro-2-azulenylbis(4-methoxyphenyl)bismuth difluoride (20a):** green solids; yield 75%; mp 124−126 °C; $^1$H NMR (DMSO-$d_6$) $\delta$ 3.84 (6H, s), 7.37 (4H, d, $J$ 8.9, ArH), 7.45 (2H, t, $J$ 9.0, AzH), 7.93 (1H, t, $J$ 9.9, AzH), 8.14 (4H, d, $J$ 8.9, ArH), 8.40 (2H, d, $J$ 9.6, AzH); $^{19}$F NMR (DMSO-$d_6$) $\delta$ −137.57 (s); UV/vis ($CHCl_3$) $\lambda_{max}$/nm ($\epsilon$) 242 (57 950), 298 (54 750), 306 (55 810), 345 (7520), 351 (7640), 369 (5110), 642 (550). Anal. Calcd for $C_{24}H_{19}BiCl_2F_2O_2$: C, 43.86; H, 2.91. Found: C, 44.20; H, 3.01.

**(1,3-Dichloro-2-azulenyl)diphenylbismuth difluoride (20b):** green solids; yield 70%; mp 152−154 °C; $^1$H NMR (DMSO-$d_6$) $\delta$ 7.51 (2H, t, $J$ 9.9, AzH), 7.65 (2H, t, $J$ 7.4, ArH), 7.83 (4H, t, $J$ 7.7, ArH), 7.99 (1H, t, $J$ 9.9, AzH), 8.23 (4H, d, $J$ 7.6, ArH), 8.47 (2H, d, $J$ 9.7, AzH); $^{19}$F NMR (DMSO-$d_6$) $\delta$ −139.85 (s); UV/vis ($CHCl_3$) $\lambda_{max}$/nm ($\epsilon$) 241 (23 300), 298 (49 700), 306 (49 700), 345 (sh, 6160), 351 (6400), 368 (4480), 642 (500). Anal. Calcd for $C_{22}H_{15}BiCl_2F_2$: C, 44.24; H, 2.53. Found: C, 44.36; H, 2.65.

**1,3-Dichloro-2-azulenylbis(4-chlorophenyl)bismuth difluoride (20c):** green solids; yield 68%; mp 144−146 °C; $^1$H NMR (DMSO-$d_6$) $\delta$ 7.51 (2H, t, $J$ 9.9, AzH), 7.90 (4H, d, $J$ 8.6, ArH), 7.99 (1H, t, $J$ 9.9, AzH), 8.25 (4H, d, $J$ 8.6, ArH), 8.46 (2H, d, $J$ 9.7, AzH); $^{19}$F NMR (DMSO-$d_6$) $\delta$ −138.98 (s); UV/vis ($CHCl_3$) $\lambda_{max}$/nm ($\epsilon$) 240 (28 440), 298 (43 200), 306 (45 310), 345 (6370), 350 (6380), 367 (4410), 642 (500). Anal. Calcd for $C_{22}H_{13}BiCl_4F_2$: C, 39.67; H, 1.97. Found: C, 39.74; H, 2.15.

**1,3-Dichloro-2-azulenylbis(4-trifluoromethylphenyl)bismuth difluoride (20d):** green solids; yield 65%; mp 139−141 °C; $^1$H NMR (DMSO-$d_6$) $\delta$ 7.50 (2H, t, $J$ 9.8, AzH), 7.98 (1H, t, $J$ 9.9, AzH), 8.19 (4H, d, $J$ 8.4, ArH), 8.43 (2H, d, $J$ 9.9, AzH), 8.49 (4H, d, $J$ 8.4, ArH); $^{19}$F NMR (DMSO-$d_6$) $\delta$ 61.16 (s, 6F), −140.40 (s, 2F); UV/vis ($CHCl_3$) $\lambda_{max}$/nm ($\epsilon$) 241 (20 430), 297 (39 160), 306 (40 080), 344 (5910), 349 (5880), 367 (4200), 644 (520). Anal. Calcd for $C_{24}H_{13}BiCl_2F_8$: C, 39.31; H, 1.79. Found: C, 39.65; H, 1.95.

**Tris(1,3-dichloro-2-azulenyl)antimony difluoride (21):** green solids; yield 94%; mp 238−240 °C; $^1$H NMR (DMSO-$d_6$) $\delta$ 7.54 (6H, t, $J$ 9.9), 8.06 (3H, t, $J$ 9.9), 8.60 (6H, d, $J$ 9.6); $^{19}$F NMR (DMSO-$d_6$) $\delta$ −97.98 (s); UV/vis ($CHCl_3$) $\lambda_{max}$/nm ($\epsilon$) 241 (45 450), 310 (138 280), 347 (sh, 19 970), 353 (21 330), 370 (16 480), 650 (1500). Anal. Calcd for $C_{30}H_{15}SbCl_6F_2$: C, 48.18; H, 2.02. Found: C, 48.26; H, 2.14.

**Bis(1,3-dichloro-2-azulenyl)phenylantimony difluoride (22):** green solids; yield 93%; mp 248−250 °C (dec); $^1$H NMR (DMSO-$d_6$) $\delta$ 7.51 (4H, t, $J$ 9.9, AzH), 7.76−7.77 (3H, m), 8.03 (2H, t, $J$ 9.9, AzH), 8.29−8.31 (2H, m), 8.54 (4H, d, $J$ 9.6, AzH); $^{19}$F NMR (DMSO-$d_6$) $\delta$ −118.27 (s); due to low solubility, measurement of $^{13}$C NMR spectrum failed; UV/vis ($CHCl_3$) $\lambda_{max}$/nm ($\epsilon$) 242 (27 600), 299 (65 830), 309 (79 170), 346 (sh, 10 640), 353 (11 650), 370 (9360), 645 (900). Anal. Calcd for $C_{26}H_{15}SbCl_4F_2$: C, 49.65; H, 2.41. Found: C, 50.08; H, 2.59.

**(1,3-Dichloro-2-azulenyl)diphenylantimony difluoride (23):** green solids; yield 91%; mp 220−222 °C; $^1$H NMR (DMSO-$d_6$) $\delta$ 7.49 (2H, t, $J$ 9.9, AzH), 7.69−7.70 (6H, m, ArH), 8.00 (1H, t, $J$ 9.9, AzH), 8.16−8.18 (4H, m, ArH), 8.47 (2H, d, $J$ 9.7, AzH); $^{19}$F NMR (DMSO-$d_6$) $\delta$ −134.31 (s); UV/vis ($CHCl_3$) $\lambda_{max}$/nm ($\epsilon$) 240 (18 600), 290 (44 090), 305 (41 110), 353 (5750), 370 (4870), 641 (520). Anal. Calcd for $C_{22}H_{15}SbCl_2F_2$: C, 51.81; H, 2.96. Found: C, 51.85; H, 2.85.

**X-ray Crystallography.** All measurements were made on a Rigaku AFC5R diffractometer with graphite-monochromated Mo Kα radiation ($\lambda$ = 0.71069 Å) and a rotating anode generator. The data were collected at 298 K using the $\omega-2\theta$ scan technique. The data were corrected for Lorentz and polarization effects. The structures were solved by the Patterson method[12] and expanded using Fourier techniques.[13] The non-hydrogen atoms were refined anisotropically. Neutral atom scattering factors were taken from Cromer and Waber.[14]

(11) Toda, T.; Yamanouchi, A. *Bull. Chem. Soc. Jpn.* **1970**, *43*, 2181.

(12) Fan, H.-F. *SAPI91*: Structure Analysis Programs with Intelligent Control; Rigaku Corporation: Tokyo, Japan, 1991.

(13) Beurskens, P. T.; Admiraal, G.; Beurskens, G.; Bosman, W. P.; de Gelder, R.; Israel, R.; Smits, J. M. M. *DIRDIF94*: The DIRDIF-94 program system, Technical Report of the Crystallography Laboratory; University of Nijmegen: The Netherlands, 1994.

(14) Cromer, D. T.; Waber, J. T. In *International Tables for X-ray Crystallography*; The Kynoch Press: Birmingham, England, 1974; Vol. IV, Table 2.2 A.

(15) Ibers, J. A.; Hamilton, W. C. *Acta Crystallogr.* **1964**, *17*, 781.

(16) Creagh, D. C.; McAuley, W. J. In *International Tables for X-ray Crystallography*; Kluwer Academic Publishers: Boston, 1992; Vol. C, Table 4.2.6.8.

(17) Creagh, D. C.; Hubbell, J. H. In *International Tables for X-ray Crystallography*; Kluwer Academic Publishers: Boston, 1992; Vol. C, Table 4.2.4.3.

(18) *TeXsan*: Crystal Structure Analysis Package; Molecular Structure Corporation, 1985 and 1999.

Anomalous dispersion effects were included in $F_{calc}$;[15] the values for $\Delta f'$ and $\Delta f''$ were those of Creagh and McAuley.[16] The values for the mass attenuation coefficients are those of Creagh and Hubbell.[17] All calculations were performed using the teXsan[18] crystallographic software package of Molecular Structure Corporation.

**Supporting Information Available:** Crystal data for compounds **7** and **20b**. This material is available free of charge via the Internet at http://pubs.acs.org.

OM040053F